Table S.1 – Overview on the adsorption energies (eV) and geometry parameters (Å) of the energetically most stable adsorption complexes. *Gas stands for the gas-phase parameters of thiophene and H-derivatives; *Ads. corresponds to adsorbed phase.

Surface	Molecule	E_{ads}		$d_{S\text{-}C^2}$	$d_{C^2\text{-}C^3}$	$d_{C^3\text{-}C^4}$	$d_{C^4\text{-}C^5}$	$d_{C^5\text{-}S}$	$d_{S\text{-}Nb}$	$d_{C^2\text{-}Nb}$	$d_{C^5\text{-}Nb}$
NbC(001)	Th	-0.42									
			Gas*	1.716	1.372	1.420	1.372	1.716	-	-	-
			Ads.*	1.727	1.367	1.428	1.367	1.725	2.808	3.941	3.946
	2-MHTh	-1.55									
			Gas	1.836	1.493	1.376	1.396	1.728	-	-	-
			Ads.	1.844	1.50 1	1.347	1.467	1.845	2.655	3.917	2.457
	2,5-DHTh	-0.70									
			Gas	1.835	1.496	1.332	1.496	1.835	-	-	-
			Ads.	2.754	1.842	1.333	1.492	1.842	2.754	3.888	3.911
NbN(001)	Th	-1.10									
			Ads.	1.852	1.474	1.366	1.479	1.861	2.642	2.387	2.386
	2-MHTh	-2.17									
			Ads.	1.843	1.498	1.349	1.462	1.851	2.764	3.495	2.369
	2,5-DHTh	-0.86									
			Ads.	1.837	1.494	1.333	1.493	1.837	2.789	3.765	3.862

Table S.2 - Reaction energy (E_R), reaction barrier (E_A), and geometric parameters at the intermediates and transition states for thiophene desulfurization reactions over niobium carbide and nitride (001) surfaces

Surface	Molecule	E_A^1	E_A^2	E_{R1}	E_{FS}		d_{S-C}^2	$d_{C}^{2}{}_{-C}^{3}$	$d_{C}^{3}{}_{-C}^{4}$	$d_{C}^{4}{}_{-C}^{5}$	$d_{C}^{5}{}_{-S}$	d_{S-Nb}	$d_{C}^{2}{}_{-Nb}$	$d_{C}^{5}{}_{-Nb}$
NbC(001)														
	Th	1.74	1.82	0.92	0.87	TS1	2.539	1.373	1.434	1.362	1.734	2.516	4.342	3.772
						RI	3.585	1.359	1.454	1.352	1.755	2.487	2.252	3.697
						TS2	3.594	1.385	1.424	1.410	2.491	2.270	2.188	2.389
						FS	3.641	1.371	1.459	1.367	3.568	2.203	2.218	2.209
	2-MHTh	1.08	2.28	-0.22	1.14	TS1	2.442	1.427	1.391	1.408	1.741	2.647	3.459	2.946
						RI	3.323	1.373	1.431	1.373	1.723	2.621	2.799	3.587
						TS2	4.146	1.353	1.451	1.420	1.952	2.445	4.272	2.522
						FS	5.195	1.345	1.446	1.358	3.521	2.210	5.360	2.226
	2,5-DHTh	1.27	0.95	-0.33	-0.16	TS1	2.587	1.430	1.349	1.491	1.816	2.597	3.294	3.863
						RI	3.331	1.453	1.360	1.505	1.842	2.489	2.401	3.709
						TS2	3.353	1.417	1.398	1.406	2.547	2.335	2.525	3.655
						FS	3.656	1.345	1.462	1.345	3.559	2.224	3.813	3.985
NbN(001)														
	Th	0.90	0.91	-0.08	-0.22	TS1	2.513	1.451	1.411	1.403	1.783	2.576	2.245	2.622
						RI	3.506	1.383	1.462	1.372	1.757	2.524	2.240	2.925
						TS2	3.929	1.348	1.333	1.353	1.997	2.415	2.178	2.473
						FS	3.559	1.371	1.469	1.373	3.573	2.206	2.219	2.231
	2-MHTh	1.08	1.27	-0.16	0.95	TS1	2.436	2.416	1.397	1.406	1.784	2.588	3.265	2.638
						RI	3.320	1.476	1.390	1.455	1.814	2.499	2.313	2.411
						TS2	3.362	1.467	1.386	1.463	2.630	2.267	2.335	2.170
						FS	3.599	1.458	1.399	1.476	3.400	2.183	2.373	1.973
	2,5-DHTh	1.07	1.02	-0.51	-0.30	TS1	2.582	1.434	1.350	1.494	1.825	2.512	3.307	3.655
						RI	3.323	1.465	1.359	1.504	1.833	2.480	2.313	3.473
						TS2	3.474	1.403	1.413	1.403	2.616	2.298	2.537	3.279
						FS	3.670	1.470	1.393	1.470	3.594	2.191	2.320	2.330

Table S.3 - Adsorption energies for twenty different Thiophene/surface structures. Bold numbers stands for the energetically most stable systems.

Surface	Position	E_{ads}	Position	E_{ads}
NbC(001)				
	Upright (η-1)		Flat (η-5)	
	1	**-0.42**	1	-0.20
	2	-0.34	2	-0.17
	3	-0.18	3	-0.24
	4	-0.15	4	0.73
	5	-0.32	5	-0.21
NbN(001)				
	Upright (η-1)		Flat (η-5)	
	1	-0.47	1	0.28
	2	-0.52	2	-0.51
	3	-0.48	3	-0.49
	4	-0.46	4	0.29
	5	-0.52	**5**	**-1.10**

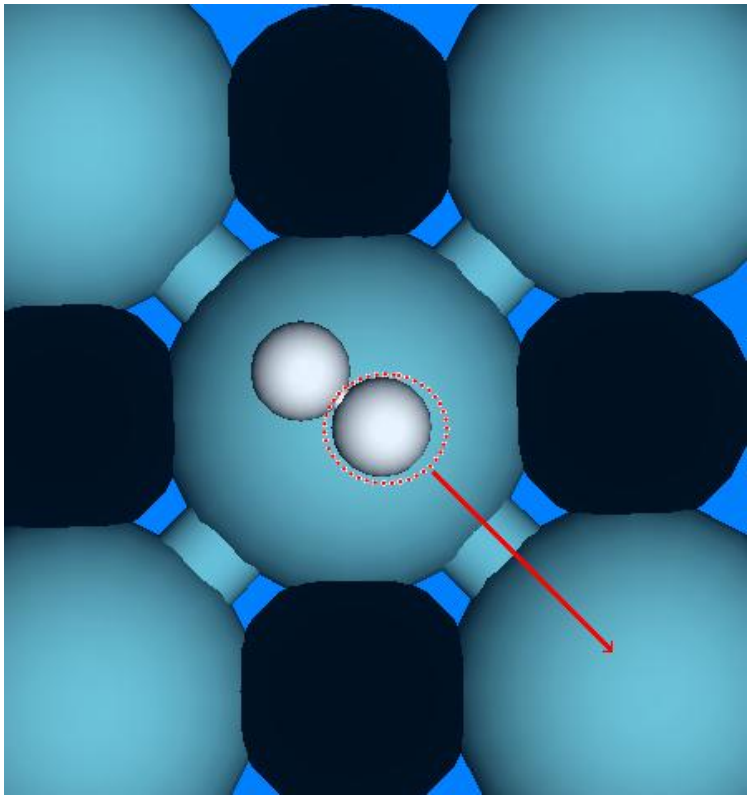

Fig S.1 - Dissociation path for the H_2 molecule over either carbide or nitride (001) surfaces.

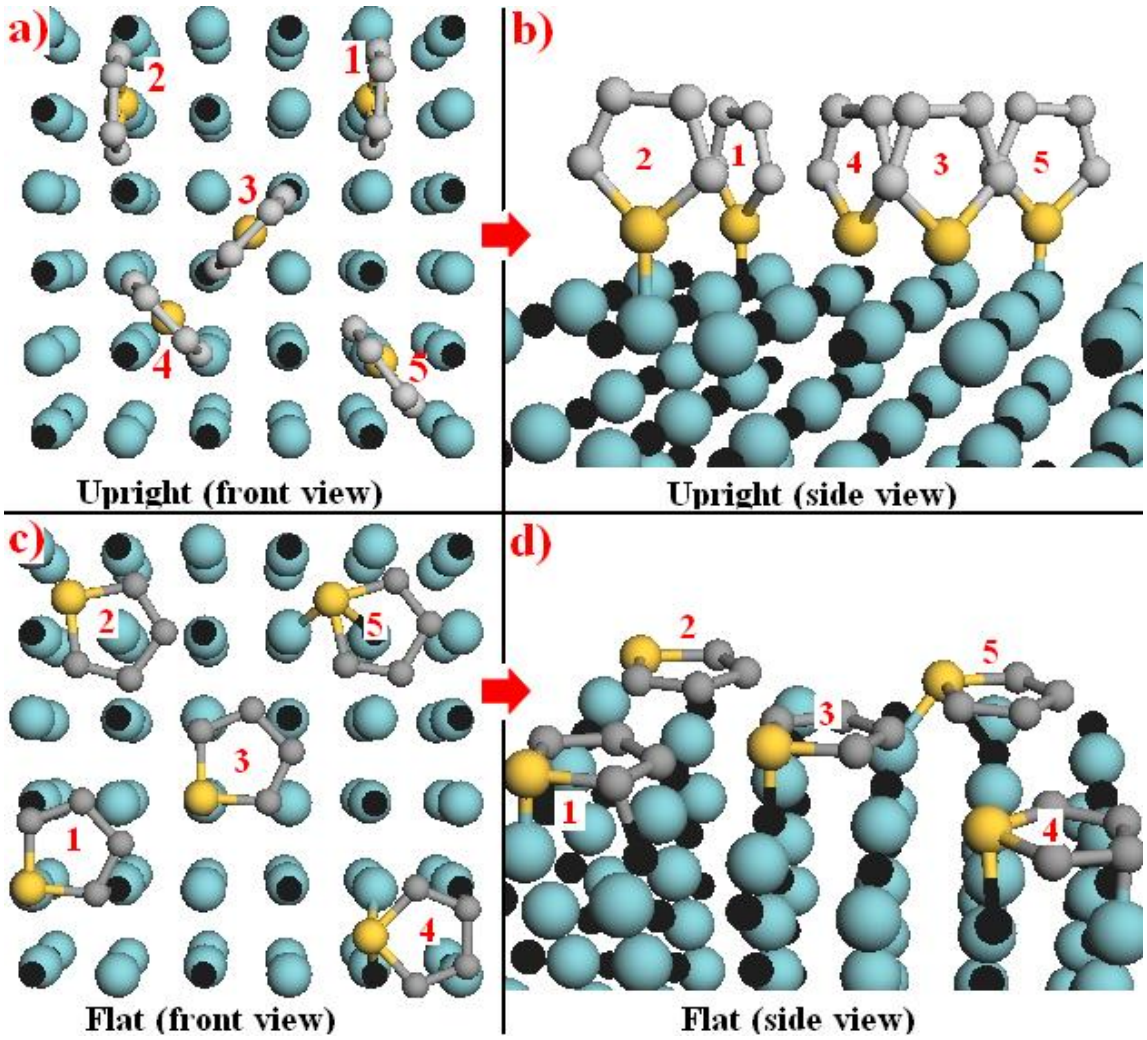

Figure S.2– Schematic configuration for the thiophene starting positions on the niobium carbide and nitride surfaces. On the systems "a" and "b" four possibilities were proposed by considering thiophene molecules in a η-1 (upright) configurations: 1) S directly bonded to an Nb atom in turn directly bonded to four Nb atoms, and the molecular ring oriented to N/C surface atoms; 2) S bonded to Nb in turn directly bonded to four N/C atoms, and ring oriented to N/C surface atoms; 3) the thiophene S atom is centered above a fourfold hollow, and ring oriented to N/C surface atoms; 4) S atom is centered above a fourfold hollow, and ring oriented to Nb surface atoms; 5) S directly bonded to an Nb atom in turn directly bonded to four N/C atoms, and ring oriented to Nb surface atoms. On the systems "c" and "d" also five possibilities have been tested with thiophene in a η-5 (flat) configuration: 1) thiophene molecular ring adsorbed on fourfold surface hollow, and S bonded to a Nb surface atom; 2) thiophene molecular ring adsorbed on a surface Nb atom, and S oriented to Nb; 3) thiophene molecular ring adsorbed on fourfold surface hollow, and S bonded to a N/C surface atom; 4) thiophene molecular ring adsorbed on fourfold surface hollow, and S oriented in between Nb and N/C surface atoms; 5) thiophene molecular ring adsorbed on a surface N/C atom, and S oriented to surface N/C atoms. The niobium, carbon and nitrogen atoms of the carbide/nitride surfaces are represented by the cyan (niobium) and black (carbon or nitrogen) balls. Furthermore, the thiophene hydrogen atoms were omitted for simplicity.

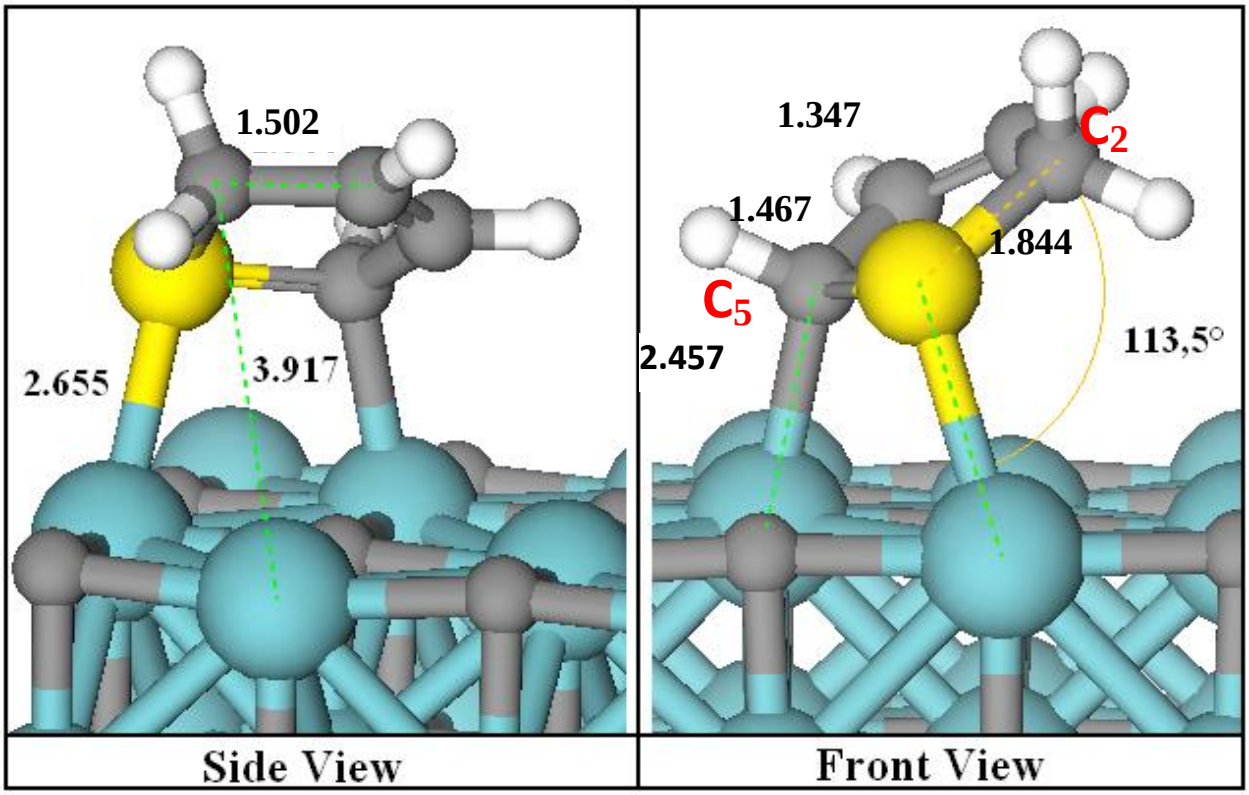

Figure S3. - Side and front view of the basic structure of 2-monohydrothiophene (2-MHTh) adsorbed on the niobium carbide surface. The numbers represent the select bond lengths (Å) as well as the angle (in degrees) between the molecular ring and the surface.

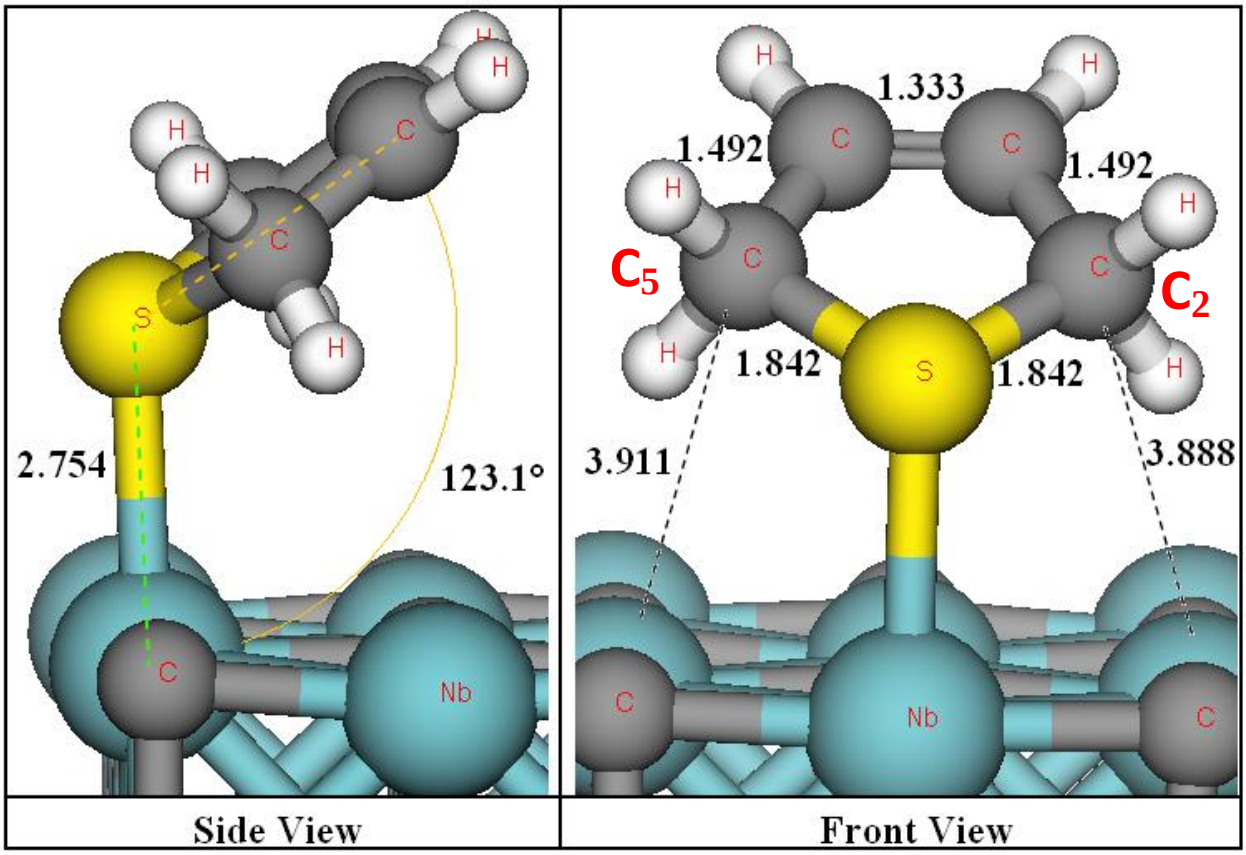

Figure S4. - Side and front view of the basic structure of 2,5-dihydrothiophene (2,5-DHTh) adsorbed on the niobium carbide surface. The numbers represent the select bond lengths (Å) as well as the angle (in degrees) between the molecular ring and the surface.

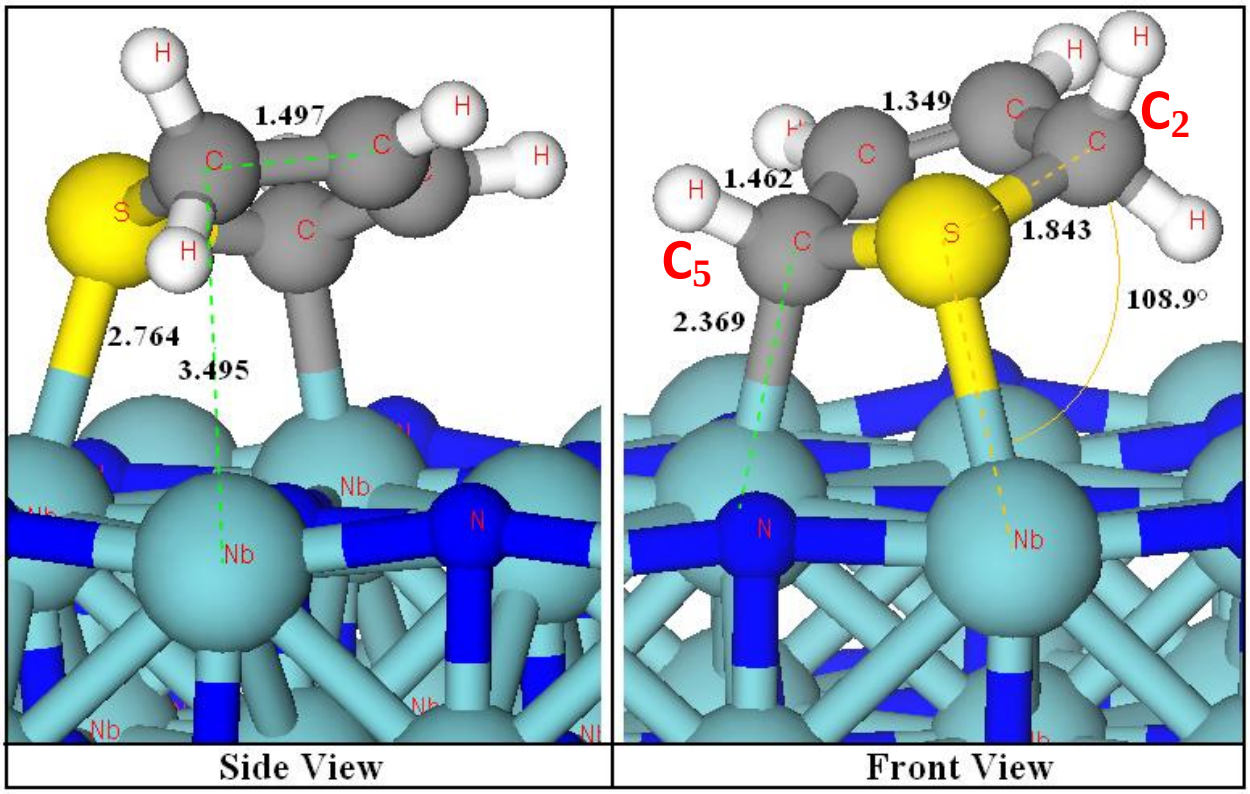

Figure S5. - Side and front view of the basic structure of 2-monohydrothiophene (2-MHTh) adsorbed on the niobium nitride surface. The numbers represent the select bond lengths (Å) as well as the angle (in degrees) between the molecular ring and the surface.

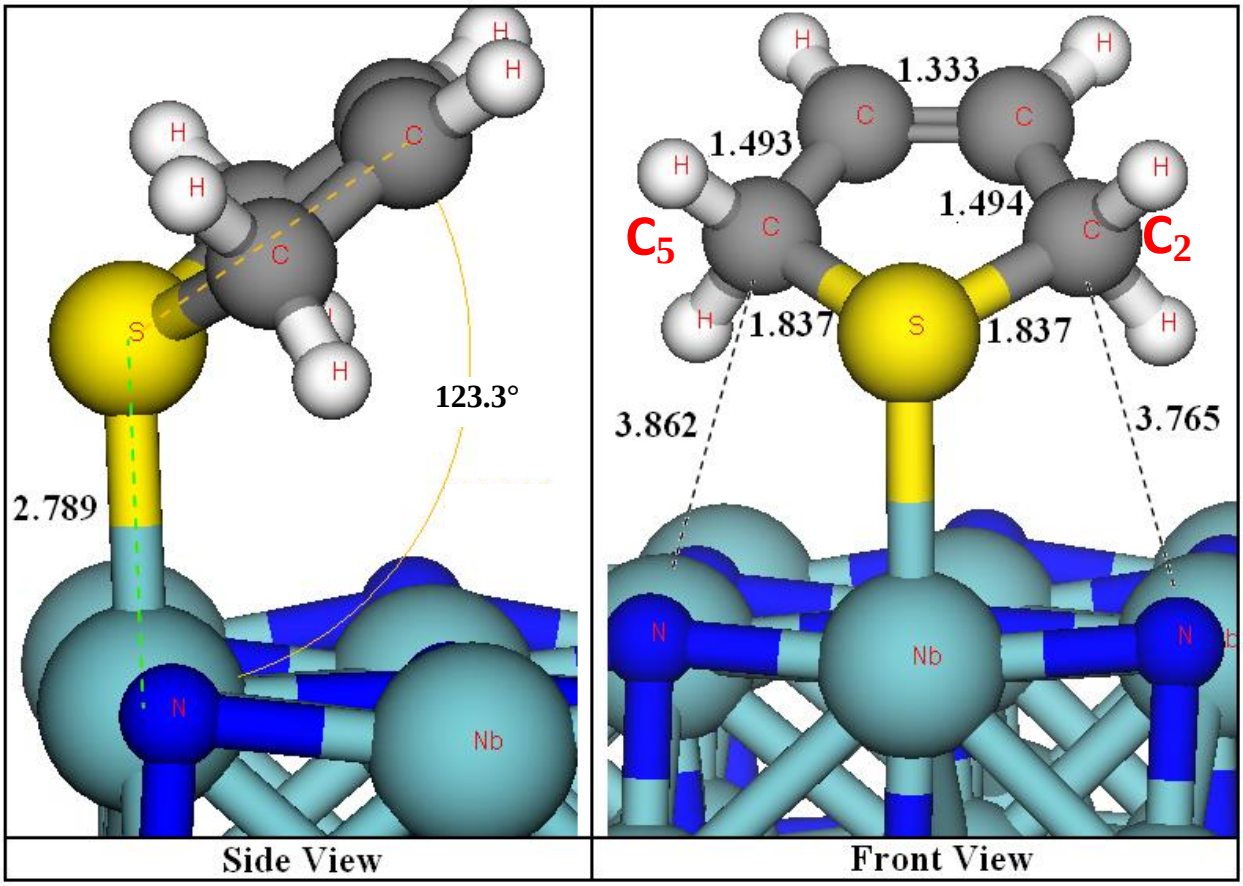

Figure S6. - Side view and front view of the basic structure of 2,5-dihydrothiophene (2,5-DHTh) adsorbed on the niobium nitride surface. The numbers represent the select bond lengths (Å) as well as the angle (in degrees) between the molecular ring and the surface.

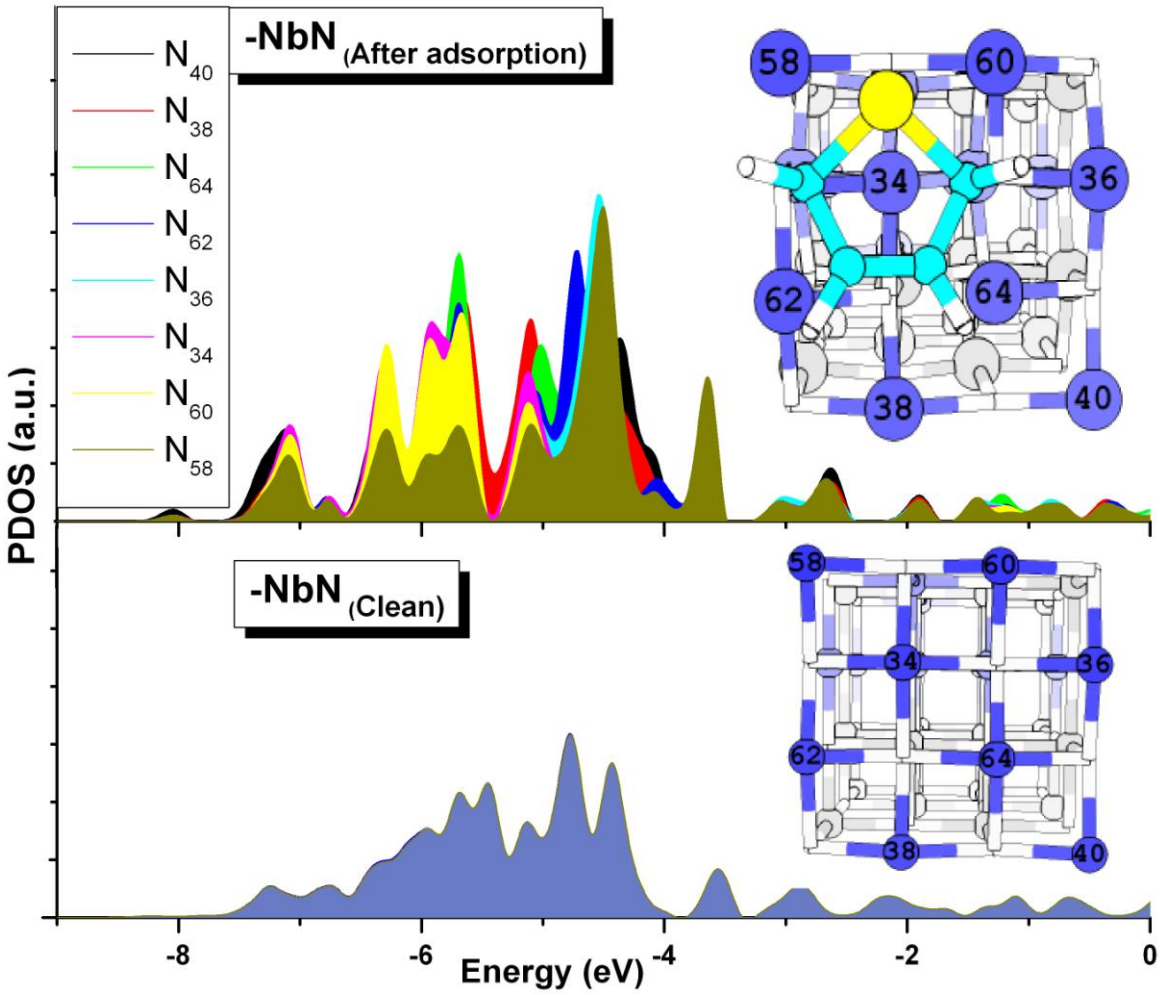

Figure S7. - Projected density of states (PDOS) of **N 2p-states** resolved for selected nitrogen atoms of the niobium nitride surface before and after (thiophene is showed for clarity) optimization. The energy scale is referred to Fermi level (set at zero).

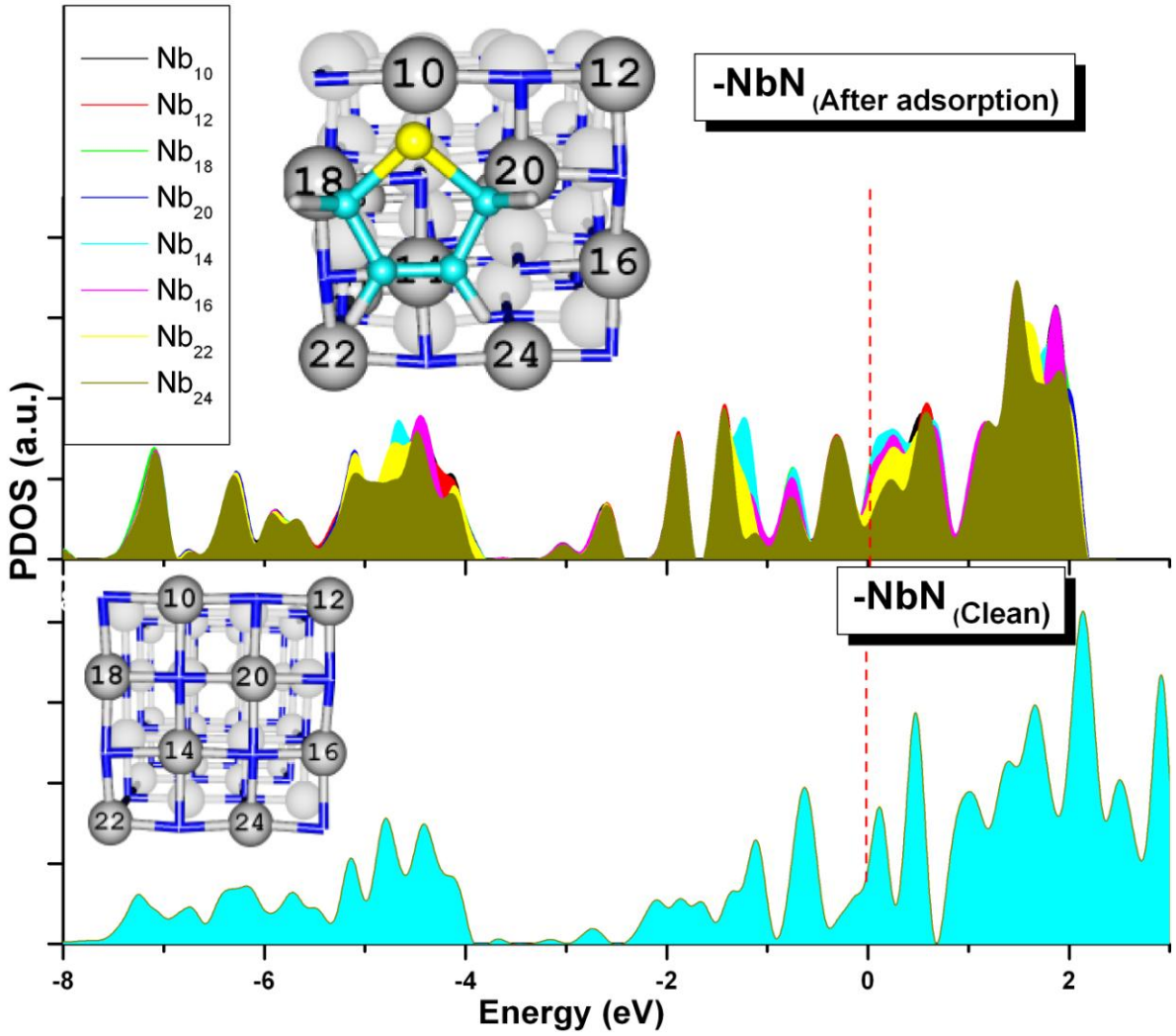

Figure S8. - Projected density of states (PDOS) of **Nb 3d-states** resolved for selected niobium atoms of the niobium nitride surface before and after (thiophene is showed for clarity) optimization. The energy scale is referred to Fermi level (dashed line).

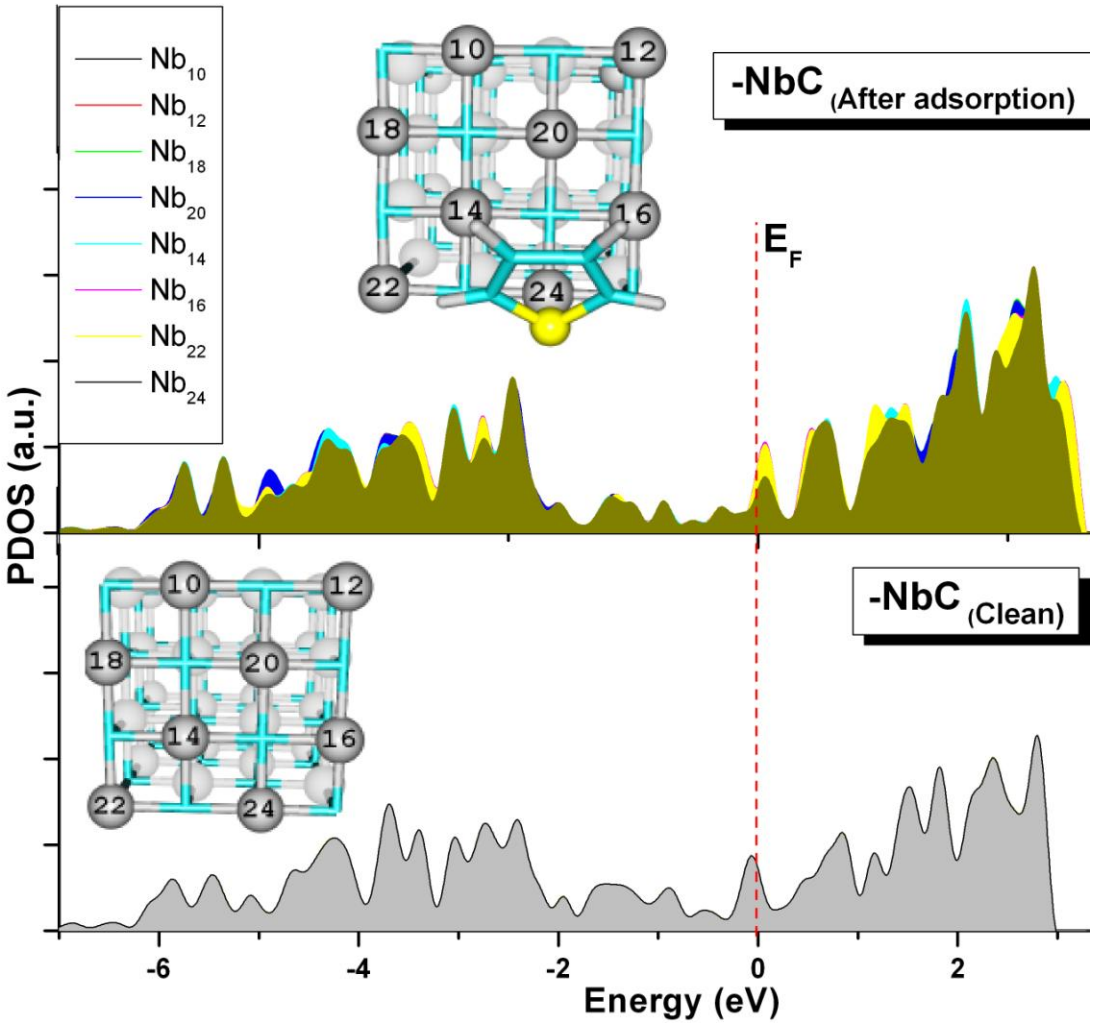

Figure S9. - Projected density of states (PDOS) of **Nb 3d-states** for selected niobium atoms of the niobium carbide surface before and after (thiophene is showed for clarity) optimization. The energy scale is referred to Fermi level (dashed line).

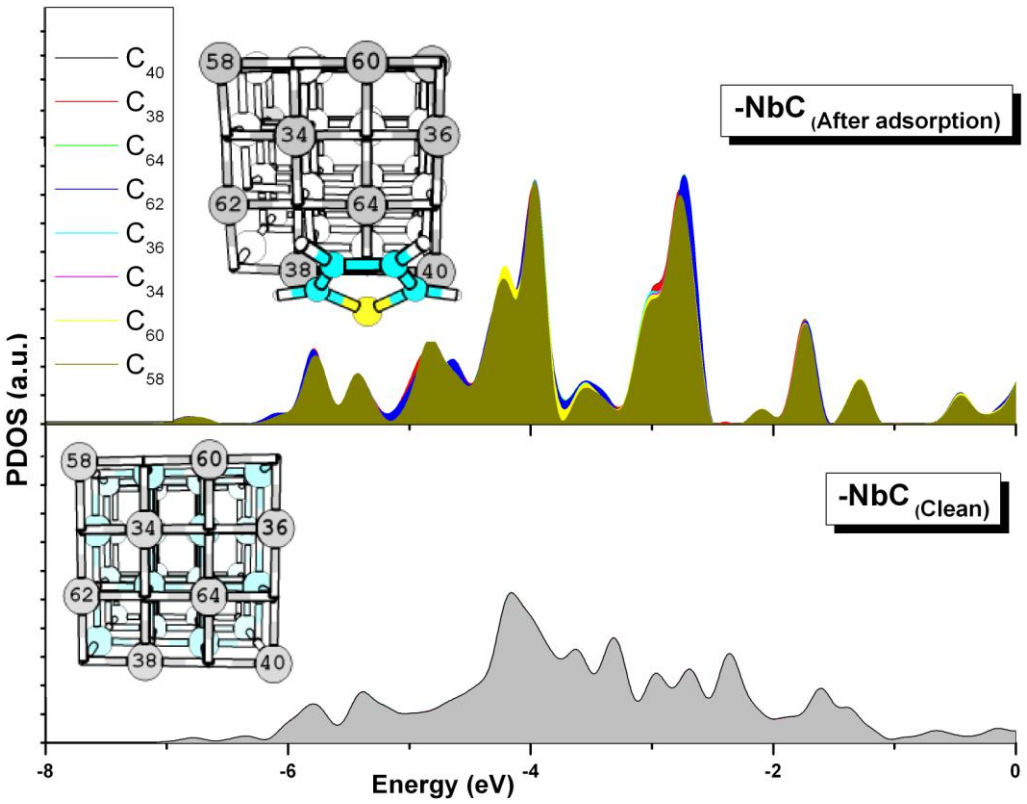

Figure S10. - Projected density of states (PDOS) of **C 2p-states** for selected carbon atoms of the niobium carbide surface before and after (thiophene is showed for clarity) optimization. The energy scale is referred to Fermi level (set at zero).

On the thiophene H-derivatives - On going from the adsorbed thiophene to the H-derivatives studied in this paper by considering realistic HDS conditions, it is conceivable that reactions of these H-species may be competing with the direct cleavage of the S-C bond in thiophene [SR.1]. It is known that the hydrogenating species are able to change the chemical structure of thiophene by gradually decreasing the ring aromaticity, in turn facilitating the S-C bond breaking via the HDS mechanism [SR.2-SR.4]. **"In order to shed light on the H_2 dissociation process and on the thiophene ring hydrogenations, a DFT study was carried out. Our calculations show that H_2 adsorbs weakly over either the carbide or nitride (001) surfaces, with the most exothermic adsorption energies of 0.26 eV and 0.41 eV for the carbide (BL_{Nb-H}= 2.173Å; BL_{H-H}=0.785Å) and nitride (BL_{Nb-H}=2.481Å; BL_{H-H}=0.764Å) surfaces, respectively, obtained when molecules are placed on a surface metal (Nb) site. From these points we evaluated the dissociation process using NEB calculations, considering that the dissociation process take one of the freshly-formed atomic hydrogens towards the nearest surface Nb site (see Fig. S.1) forming strong Nb-H bonds. Other possibilities for the H_2 dissociation were not evaluated in the present paper and will be left for the future works. We found that on the nitride surface, despite the weak adsorption energy (0.41 eV), the dissociation of the H_2 molecule accounts for a barrier of 0.38 eV, indicating a preference for further dissociation rather than desorption. On the other hand, apart from the lower adsorption energy of H_2 (0.26 eV), we found a considerably high dissociation barrier of 1.44 eV, which indicates that on the NbC(001) surface a hydrogen molecule tends to desorb rather than dissociate. This is a surprisingly high energy barrier, but as mentioned previously the diffusion to the nearest Nb site was considered (see Fig. S.1), and it might have been hampered by the rippling of the C atoms induced by the relaxation of the surface (see section 3.1 in the main article).**

In principle, from these results it would be possible to imply that the NbN(001) surface has a better hydrogenation ability when compared to NbC(001). Accordingly, we have now examined the

hydrogenation of thiophene and for simplicity we assumed that the atomic hydrogens are available on the Nb sites (Nb-H). Moreover, we have only considered the formation of the 2-MHTh/surface and 2,5-DHTh/surface systems from the first 1st and 2nd hydrogenations of thiophene (C^2 and C^5 atoms), respectively. Thus, for the carbide surface we observed that the first step to form the 2-MHTh/NbC(001) (Fig. S.3) adsorption complex has a barrier of 1.51 eV, whereas the same hydrogenation step in 2-MHTh/NbN(001) (Fig. S.5) has an energy barrier of 2.05 eV. The second addition of H to the ring C^5 atom to form the 2,5-DHTh/NbC(001) (Fig. S.4) system accounts for an energy barrier of 1.64 eV, whereas the same reaction over NbN(001) (Fig. S.6) has an energy barrier of 1.77 eV.

Interestingly, we observed that though the dissociation of H_2 should probably be easier to occur on the nitride surface than on the carbide surface, in a hypothetic situation in which a H_2 molecule would be readily dissociated, the thiophene ring hydrogenation on the carbide surface would have slightly lower activation barriers than on the nitride for both the 1st and 2nd hydrogenations. Nevertheless, our results clearly show that this feature does not substantially improve the desulfurization efficiency of the carbide surface when compared to nitride (see from the section 3.2 onwards in the main article).” This apparently controversial result might be explained by the fact that the thiophene ring in the partially tilted η-1 configuration on carbide surface be able to expose a larger area to the attack of the hydrogenating species in comparison with the η-5 configuration of nitride. The tilted structure of the η-1 configuration increases the number of possible directions of approximation and the frequency of collision of the hydrogenating species with thiophene, resulting in better hydrogenating ability of the carbide surface. These results are closely related with those reported for the thiophene H-derivatives over Pt(111) and Pt(110) [SR.8,SR.9]. Furthermore, the hydrogenation process has approximately the same effect over the nitride and the carbide surfaces with respect to the modification of the S-C and C-C bonds of the 2-MHTh and the 2,5-DHTh species. The calculated adsorption energies show that the formation of the hydrogenated species is exothermic on both surfaces. It is

also important to mention that according to experiments the hydrogenation of aromatic molecules in the gas phase is usually a highly endothermic process and for that reason the interaction with the surface would stabilize the systems under study [SR.5]. Subsequent hydrogenations to form tetrahydrothiophene (THT) were not explored in the present paper because, as shown in the literature, under realistic HDS conditions THT has equilibrium limitations and it is possibly an intermediate only at high H_2 pressure and low temperatures [SR.6,SR.7]. In an interesting case, Moses and collaborators [SR.2] found that the hydrogenation of thiophene on Co-promoted molybdenum sulfides is preferred on both Mo and S edges in comparison with the direct cleavage and that 2,5-DHTh is the most important specie formed, although the whole desulfurization process involves multiple intermediates. This specie is formed by the second hydrogenation of 2-MHTh, which is a chemically unstable specie and not observed experimentally [SR.2].

On the limitations of the models **–** The desulfurization of an aromatic molecule like thiophene is quite a complex process and, although the reaction mechanism is not fully understood even on common used catalysts, under realistic conditions it might include more steps than those accounted for in the present work [SR.10]. However, as reported by different authors the features of the adsorption of thiophene and its hydrogenated derivatives play an essential role during the desulfurization process, principally due to the change of bond strength caused by the adsorption which may be correlated to reactivity [SR.11-SR.16]. In addition, other intermediates, reaction products and arrangements of possible co-existing species [SR.17] were not investigated in the present paper, which might be an artificial viewpoint of the catalytic process. Turning now to the catalyst side, one of the main drawbacks dealing with TMCNs is the presence of surface vacancies not taken into account into the models. From a thermodynamic viewpoint the existence of perfect catalytic surfaces is impossible due to the inevitable occurrence of non-stoichiometric imperfections and defects, which has enormous effects on the catalytic properties of these surfaces [SR.22]. It is known that cubic (Fm3m) TMCNs are able to accommodate a large number of non-metal vacancies (up to about 50%) while still retaining its

crystalline structure [SR.20]. These vacancies might as well be correlated to reactivity, since it is known that catalytic processes commonly occur in defects of this type on the surface [SR.17]. Moreover, the synthesis of TMCNs is usually difficult requiring elevated temperatures and long reaction times, which might affect the number of active sites for various reasons *e.g.* sintering poisoning, solid-state transformation coking, etc. [SR.17-SR.19], which in turn might alter the reaction energies and activation barriers. Moreover, especially in the case of nitride surfaces, both the nitrogen vacancy formation and the adsorption and structural transformations of thiophene on a sulfided surface is a real possibility, as shown by experiments [SR.21], with consequences on the activation energies [SR.14]. Obviously, we are not aiming to provide a complete mechanism for the desulfurization of thiophene over niobium carbide and nitride surfaces; much less we are implying that the reaction pathway is determined precisely by the steps proposed in this work. However, these reaction steps are well known in the literature and are among the most studied due to the great importance of the desulfurization processes. They consist of distinct species (hydrocarbon intermediates) with varying H content which should hold for different transformations of thiophene. Thus, the organic species proposed during desulfurization reactions comprises a small part in a plethora, as observed experimentally, by other authors.

REFERENCES

[SR.1] Topsøe, H.; Clausen, B.S.; Massoth, F.E. Hydrotreating Catalysis, Science and Technology, Springer, New York, 1991.

[SR.2] Moses, P.G.; Hinnemann, B.; Topsøe, H.; Nørskov, J.K. Journal of Catalysis 248 (2007) 188–203.

[SR.3] Tominaga, H., Nagai, M., Applied Catalysis A: General 343 (2008) 95.

[SR.4] Zhu, H.; Guo, W.; Li, M.; Zhao, L.; Li, S.; Li, Y.; Lu, X.; Shan, H.; ACS Catal. 1 (2011) 1498.

[SR.5] Mittendorfer, F and Hafner, J. J. Phys. Chem. B 2002, 106, 13299-13305.

[SR.6] Vrinat, M.L. Applied Catalysis, 6 (1983) 137-158.

[SR.7]Moses, P.G.; Hinnemann, B.; Topsøe, H.; Nørskov, J.K. Journal of Catalysis 268 (2009) 201–208.

[SR.8] Zhu, H.; Guo, W.; Li, M.; Zhao, L.; Li, S.; Li, Y.; Lu, X.; Shan, H.; ACS Catal. 1 (2011) 1498.

[SR.9] Zhu, H.; Lu, X.; Guo, W.; Li, L.; Zhao, L.; Shan, H. Journal of Molecular Catalysis A: Chemical 363–364 (2012) 18–25.

[SR.10] Topsøe, H.; Clausen, B.S.; Massoth, F.E. Hydrotreating Catalysis, Science and Technology, Springer, New York, 1991.

[SR.11] Moses, P.G.; Hinnemann, B.; Topsøe, H.; Nørskov, J.K. Journal of Catalysis 248 (2007) 188.

[SR.12] Mittendorfer, F.; Hafner, J. Surf. Sci. 492 (2001) 27.

[SR.13] Mittendorfer, F.,Hafner, J., Journal of Catalysis 214 (2003) 234.

[SR.14] Tominaga, H., Nagai, M., Applied Catalysis A: General 343 (2008) 95.

[SR.15] Zhu, H.; Guo, W.; Li, M.; Zhao, L.; Li, S.; Li, Y.; Lu, X.; Shan, H.; ACS Catal. 1 (2011) 1498.

[SR.16] Zhu, H.; Lu, X.; Guo, W.; Li, L.; Zhao, L.; Shan, H. Journal of Molecular Catalysis A: Chemical 363 (2012) 18.

[SR.17] Ramanathan, S; Oyama, S.T. J. Phys. Chem. 99 (1995) 16365.

[SR.18] Schwartz, V.; Oyama, S. T.; Chen, J.C. J. Phys. Chem. B 104 (2000) 8800-8806.

[SR.19] Forzatti, P.; Lietti, L. Catal.Today 52 (1999) 165-181.

[SR.20] Toth, L.E. Transition Metal Carbides and Nitrides Academic Press, New York (EE.UU.) (1971).

[SR.21] Nagai, M.; Nakauchi, R.; Ono, Y.; Omi, S. Catal. Tod. 57 (2000) 297.

[SR.22] Swalin, R.A., Themodynamics of Solids. Wiley, New York, 1972.